Free Vibration and Bending Behaviour of CNT Reinforced Composite Plate using Different Shear Deformation Theory

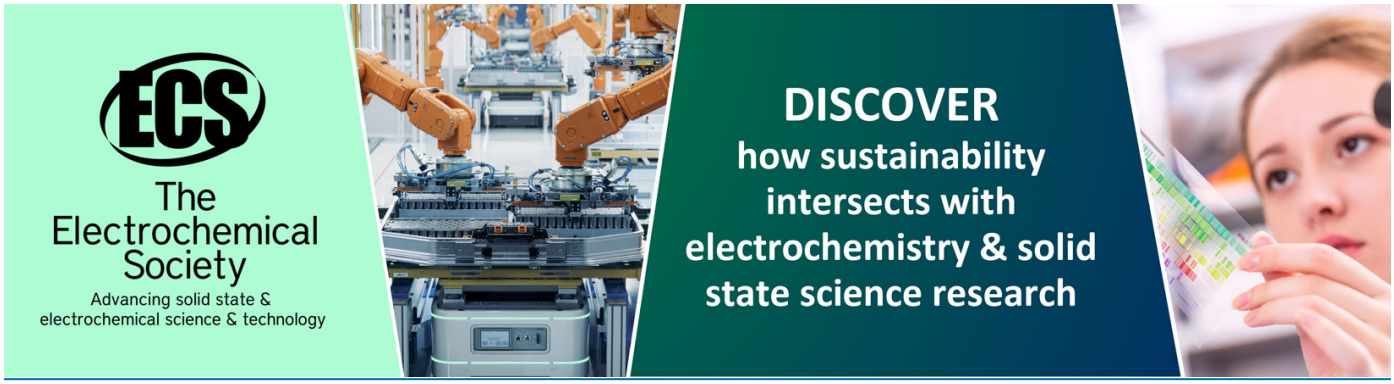

IOP Conf. Series: Materials Science and Engineering **115** (2016) 012014 doi:10.1088/1757-899X/115/1/012014

Free Vibration and Bending Behaviour of CNT Reinforced Composite Plate using Different Shear Deformation Theory

K Mehar* **and S K Panda**

Department of Mechanical Engineering, National Institute of Technology Rourkela. India.

*E-mail:kulmanimehar@gmail.com

Abstract. In the present study, the free vibration and the bending behaviour of carbon nanotube reinforced composite plate are computed using three different shear deformation theories under thermal environment. The material properties of carbon nanotube and matrix are assumed to be temperature-dependent, and the extended rule of mixture is used to compute the effectivematerial properties of the composite plate. The convergence and validity of the present modelalso have been checked by computing the wide variety of the numerical example. The applicability of the proposed higher-order models has been highlighted by solving the wide variety of examples for different geometrical and material parameters underelevated thermal environment.The responses are also examined using the simulation model developed in commercial finite element package (ANSYS).

Keywords: CNT, free vibration, bending, thermal environment,FSDT,HSDT.

1. Introduction

From last few decade, many types of researchhave already been completedon the fibre or the laminated composite materials to show the significant improvementof the specific strength and the stiffness behaviour of the advanced structure or the structural components. Recently, carbon nanotubes (CNTs) are used as the reinforcement material in nanocomposites due to their excellent specific strength, specific stiffness, thermal, electrical, and chemical properties. The CNT has got numerous applications in the aerospace, the nuclear plant, automobile and marine structures due to their outstanding properties. The effective material properties of the carbon nanotube reinforced composite (CNTRC) are evaluated using the variousavailable method such as molecular dynamics (MD) simulation, [1-3] representative volume element (RVE) [4-5],the rule of mixture [6-7] and Eshelby–Mori–Tanaka approach [8].In general, the CNTs are classified based on their configurations namely, armchair, zigzag and chiral and their elastic properties varyaccordingly. Ayatollahia *et al*. [9] estimated the nonlinear mechanical properties of the single wall nanotubes under three different set of load (tensile, bending and torsional load) using a molecular model based on the finite element method (FEM) for both armchair and zigzag configuration.Aragh*et al*.[10] computed the free vibration behaviour of randomly oriented CNTRC cylindrical shell based on third-order shear deformation theory (TSDT). Lin and Xiang [11] investigated the free vibration response of FG-CNTRC beam using the p-Ritz method based on the first-order shear deformation theory (FSDT) and TSDT kinematic model with von Karman sense geometric nonlinearity. Shen *et al*.[12] investigated the vibration response of multi-wall carbon nanotube (MWCNT) based biosensor using nonlocal

Timoshenko beam theory(TBT).K*eet al.*[13] computed the dynamic stability, free vibration and buckling behaviour of functionally graded carbon nanotube reinforced composite (FG-CNTRC) beam using TBT. Alva and Raja [14]examined the effects of the weight percentage and the diameter of the MWCNT on the damping characteristics of the MWCNT/epoxy composite. Jarali*et al.*[15]reported the effect of agglomeration and the volume fractions on the mechanical, thermal, electrical and the moisture properties of the CNT/epoxy composite. Vodenitcharova and Zhang[16] computed the local buckling, and the bending behaviour of the SWCNT reinforced composite plates using Airy'sstress function. Formica *et al*. [17]numericallysolved the free vibration responses of the CNTRC plate using FEM and the effective material properties of the CNTRCplate are computed based on Mori-Tanaka scheme. Zhu *et al*. [18] examined the free vibration and bending analysis of the FG-CNTRC plate using the FSDT kinematics. Yas and Heshmati[19] estimated the free and force vibrational behaviour of functionally graded nanocomposite beams reinforced by randomly oriented straight SWCNTs based on Timoshenko and Euler–Bernoulli beam theories using FEM. Lei *et al*. [20-22] computed the free vibration and the buckling behaviour of the FG-CNTRC cylindrical panels based on the FSDT shell theory using the element-freekp-Ritz method. Alibeigloo and Liew[23] examined the flexural behaviour of FG-CNTRC rectangular plate with all edges simply supported boundary conditions based on the three-dimensional theory of elasticity. Lei *et al*. [24] evaluated the flexural strength and free vibration behaviour of FG-CNTR cylindrical shell panels based on the FSDT. Mehrabadi and Aragh[25] computed the static response of FG-CNTRC cylindrical shell panel using TSDT.

From the above review, weconcluded that considerable amount of work has already been completed on the property evaluation of the CNT and the CNT reinforced composites. In addition to that the structuralanalysis(free vibration, bending and buckling) of the CNT reinforced composites are computed using the FSDT kinematics with and without temperature load. Based on the authors' knowledge no study has been reportedyet on the free vibration and bending behaviour of the CNTRCplate under thermal environmentusing the HSDT kinematic model. The objective of the present work is to compute the free vibration and the bending responses of the CNTRCflat panel numerically using the FSDT and HSDT mid-plane kinematics in conjunction with FEM. The domain is discretized using the suitable isoparametric finite element steps through a nine noded element with nine (model 1), six (model) or ten (model 3) degrees of freedom (DOF) per node. The responses are obtained numerically through a customized computer code developed in MATLAB environment. The validity and the convergence behaviour of the present numerical model have been checked, and the responses are also computed usingthe simulation model developed in ANSYS through ANSYS parametric design language (APDL) code. Finally, the effect of various design parameters (aspect ratios, support conditions, thickness ratios, volume fractions and temperature load) on the free vibration, static, stress and deformation behaviour of the CNTRC plate are highlighted by solving the wide variety of examples.

2. Theory and Formulation

In this analysis, the rectangular configuration of CNTRC plate is considered for the free vibration and the bending analysis as shown in fig. 1. The dimensions of CNTRC plate are the length (*a*), width (*b*) and the thickness (*h*). The CNTs are assumed to be uniformly distributed and alignalong the length of the plate.The displacement field kinematics within the plate is assumed to be based on the HSDT/FSDT, where the in-plane displacements are expanded as cubic/linear functions of the thickness coordinate while the transverse displacement varies either linearly and/or constant through the plate thickness. In this study, three different kinematic models have been utilized for the analysis purpose and discussed in the following lines.

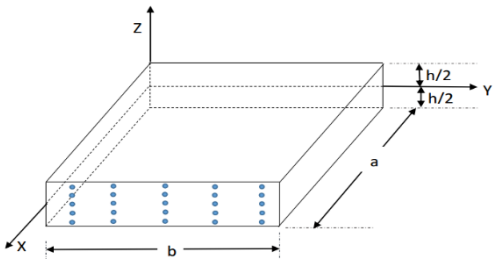

Fig. 1:- Carbon nanotube reinforced composite plate geometry and configuration.

Model 1

As a first step, the mathematical model is developed using the HSDT mid-plane kinematics with nine DOF of the CNTRCs plate as in Kishore *et al.* [26]:

$$\left.\begin{aligned} u(x,y,z,t) &= u_0(x,y,t) + z\varphi_x(x,y,t) + z^2\psi_x(x,y,t) + z^3\theta_x(x,y,t) \\ v(x,y,z,t) &= v_0(x,y,t) + z\varphi_y(x,y,t) + z^2\psi_y(x,y,t) + z^3\theta_y(x,y,t) \\ w(x,y,z,t) &= w_0(x,y,t) \end{aligned}\right\} \quad (1)$$

Model 2

Similarly, one another mathematical model is developed using the FSDT mid-plane kinematics with six DOF of the CNTRCs plate as in Szekrenyes[27]:

$$\left.\begin{aligned} u(x,y,z,t) &= u_0(x,y,t) + z\varphi_x(x,y,t) \\ v(x,y,z,t) &= v_0(x,y,t) + z\varphi_y(x,y,t) \\ w(x,y,z,t) &= w_0(x,y,t) + z\varphi_z(x,y,t) \end{aligned}\right\} \quad (2)$$

Model 3

Further, the mathematical model is developed using another HSDT mid-plane kinematics with ten DOF of the CNTRCs plate as in Kishore *et al.*[26]:

$$\left.\begin{aligned} u(x,y,z,t) &= u_0(x,y,t) + z\varphi_x(x,y,t) + z^2\psi_x(x,y,t) + z^3\theta_x(x,y,t) \\ v(x,y,z,t) &= v_0(x,y,t) + z\varphi_y(x,y,t) + z^2\psi_y(x,y,t) + z^3\theta_y(x,y,t) \\ w(x,y,z,t) &= w_0(x,y,t) + z\varphi_z(x,y,t) \end{aligned}\right\} \quad (3)$$

where, *u*, *v*, and *w* are the displacement of any point within the plate along X, Y and Z directions, respectively. u_0, v_0, and w_0 are midpoint displacement along X, Y, and Z direction respectively. φ_x and φ_y are the rotation of normal to the mid-plane about the Y and X direction respectively. φ_z, ψ_x, ψ_y, θ_x and θ_y are higher-order terms of Tayler series expansion in the mid plane of the plate.

Again, Eqs.(1), (2) and (3) are rewritten in the matrix form as follows:

$$\{\lambda\} = [f_n]\{\lambda_{0n}\} \quad (4)$$

where, $\{\lambda\}$, $[f_n]$ and $\{\lambda_{0n}\}$ are the displacement field vector of any point, thickness coordinate matrix and displacement field vector within the mid-plane of n^{th} model. The details of each term are provided in the Appendix.

The mid-plane kinematics of the CNTRC plateis evaluated using the following strain-displacement relation:

$$\{\varepsilon\}=\begin{Bmatrix}\varepsilon_{xx}\\ \varepsilon_{yy}\\ \varepsilon_{zz}\\ \gamma_{yz}\\ \gamma_{zx}\\ \gamma_{xy}\end{Bmatrix}=\begin{Bmatrix}\dfrac{\partial u}{\partial x}\\ \dfrac{\partial v}{\partial y}\\ \dfrac{\partial w}{\partial z}\\ \dfrac{\partial v}{\partial z}+\dfrac{\partial w}{\partial y}\\ \dfrac{\partial u}{\partial z}+\dfrac{\partial w}{\partial x}\\ \dfrac{\partial u}{\partial y}+\dfrac{\partial v}{\partial x}\end{Bmatrix}=\begin{Bmatrix}\varepsilon_x^0\\ \varepsilon_y^0\\ \varepsilon_z^0\\ \gamma_{yz}^0\\ \gamma_{zx}^0\\ \gamma_{xy}^0\end{Bmatrix}+z\begin{Bmatrix}\varsigma_x\\ \varsigma_y\\ \varsigma_z\\ \varsigma_{yz}\\ \varsigma_{zx}\\ \varsigma_{xy}\end{Bmatrix}+z^2\begin{Bmatrix}\zeta_x\\ \zeta_y\\ \zeta_z\\ \zeta_{yz}\\ \zeta_{zx}\\ \zeta_{xy}\end{Bmatrix}+z^3\begin{Bmatrix}\xi_x\\ \xi_y\\ \xi_z\\ \xi_{yz}\\ \xi_{zx}\\ \xi_{xy}\end{Bmatrix} \tag{5}$$

or $$\{\varepsilon\}=[T]\{\bar{\varepsilon}\} \tag{6}$$

where,

$$\{\bar{\varepsilon}\}=\left[\varepsilon_x^0\ \varepsilon_y^0\ \varepsilon_z^0\ \varepsilon_{yz}^0\ \varepsilon_{zx}^0\ \varepsilon_{xy}^0\ \varsigma_x\ \varsigma_y\ \varsigma_z\ \varsigma_{yz}\ \varsigma_{zx}\ \varsigma_{xy}\ \zeta_x\ \zeta_y\ \zeta_z\ \zeta_{yz}\ \zeta_{zx}\ \zeta_{xy}\ \xi_x\ \xi_y\ \xi_z\ \xi_{yz}\ \xi_{zx}\ \xi_{xy}\right]^T$$

$$[T]=\begin{bmatrix}1&0&0&0&0&0&z&0&0&0&0&0&z^2&0&0&0&0&0&z^3&0&0&0&0&0\\ 0&1&0&0&0&0&0&z&0&0&0&0&0&z^2&0&0&0&0&0&z^3&0&0&0&0\\ 0&0&1&0&0&0&0&0&z&0&0&0&0&0&z^2&0&0&0&0&0&z^3&0&0&0\\ 0&0&0&1&0&0&0&0&0&z&0&0&0&0&0&z^2&0&0&0&0&0&z^3&0&0\\ 0&0&0&0&1&0&0&0&0&0&z&0&0&0&0&0&z^2&0&0&0&0&0&z^3&0\\ 0&0&0&0&0&1&0&0&0&0&0&z&0&0&0&0&0&z^2&0&0&0&0&0&z^3\end{bmatrix}$$

here, [*T*] and $\{\bar{\varepsilon}\}$ are the thickness coordinate matrix and the mid-plane strain vector, respectively. The general stress-strain relationship of the composite is expressed as follows:

$$\begin{Bmatrix}\sigma_{xx}\\ \sigma_{yy}\\ \tau_{xy}\\ \tau_{zx}\\ \tau_{yz}\end{Bmatrix}=\begin{bmatrix}Q_{11}&Q_{12}&0&0&0\\ Q_{21}&Q_{22}&0&0&0\\ 0&0&Q_{66}&0&0\\ 0&0&0&Q_{55}&0\\ 0&0&0&0&Q_{44}\end{bmatrix}\left(\begin{Bmatrix}\varepsilon_{xx}\\ \varepsilon_{yy}\\ \gamma_{xy}\\ \gamma_{zx}\\ \gamma_{yz}\end{Bmatrix}-\begin{Bmatrix}\alpha_{11}\\ \alpha_{22}\\ 0\\ 0\\ 0\end{Bmatrix}\Delta T\right) \tag{7}$$

where, $Q_{11}=Q_{22}=E/(1-\upsilon^2)$, $Q_{12}=Q_{21}=E\upsilon/(1-\upsilon^2)$, $Q_{66}=Q_{55}=Q_{44}=E/2(1+\upsilon)$

In which we assumed that $G_{13}=G_{12}$ and $G_{23}=1.2\times G_{12}$. ΔT is the uniform temperature rise across the panel thickness.Eq. (7) can also be rewritten as

$$\{\sigma\}=[Q]\{\varepsilon-\varepsilon_{th}\} \tag{8}$$

where, [Q] is the reduced stiffness matrix.

Theeffective material properties of CNTRC plate can be computed using the extended rule of mixture as[18]:

$$E_{11} = \eta_1 V_{CNT} E_{11}^{CNT} + V_m E^m \tag{9}$$

$$\frac{\eta_2}{E_{22}} = \frac{V_{CNT}}{E_{22}^{CNT}} + \frac{V_m}{E^m} \tag{10}$$

$$\frac{\eta_3}{G_{12}} = \frac{V_{CNT}}{G_{12}^{CNT}} + \frac{V_m}{G^m} \tag{11}$$

and, $$V_{CNT} + V_m = 1 \tag{12}$$

where, E_{11}, $E_{22,}$and G_{12} are the effective Young's modulus in the longitudinal and lateral direction and shear modulus of CNTRCplate respectively. Similarly, E_{11}^{CNT}, E_{22}^{CNT} and G_{12}^{CNT} are the properties of the CNT in their corresponding directions. In addition, E^m and G^m are the Young's modulus and shear modulus of the matrix material respectively and η_1, η_2 and η_3 are the effective parameter of CNT in the material directions.

The effective Poisson's ratio (v_{12}) and the density of each constituent material (ρ) areobtained using the formulas as [18]:

$$v_{12} = V_{CNT} v^{CNT} + V_m v^m \tag{13}$$

$$\rho = V_{CNT}\, \rho^{CNT} + V_m \rho^m \tag{14}$$

where, v^{CNT} and v^m are Poisson's ratio of the SWCNT and the matrix material, respectively. Similarly, ρ^{CNT} and ρ^m arethe densities of the CNT and the matrix, respectively.

2.1. Finite Element Method

FEM has been widely appreciated numerical tool for the structural analysis with various geometrical and the material complexities. In this present analysis, the displacement fields for different assumed kinematic models are expressed in terms of desired field variables and the models are discretized using suitable FEM steps. The displacement vector $\{\lambda_0\}$ at any point within the mid-surface is given by:

$$\{\lambda_0\} = \sum_{i=1}^{9} N_i \{\lambda_{0i}\} \tag{15}$$

where, $\{\lambda_{0i}\} = \left[u_{0_i}\ v_{0_i}\ w_{0_i}\ \varphi_{x_i}\ \varphi_{y_i}\ \psi_{x_i}\ \psi_{y_i}\ \theta_{x_i}\ \theta_{y_i}\right]^T$, $\{\lambda_{0i}\} = \left[u_{0_i}\ v_{0_i}\ w_{0_i}\ \varphi_{x_i}\ \varphi_{y_i}\ \varphi_{z_i}\right]^T$ and $\{\lambda_{0i}\} = \left[u_{0_i}\ v_{0_i}\ w_{0_i}\ \varphi_{x_i}\ \varphi_{y_i}\ \varphi_{z_i}\ \psi_{x_i}\ \psi_{y_i}\ \theta_{x_i}\ \theta_{y_i}\right]^T$ are the nodal displacement vector formodel 1, model 2 and model 3 respectivelyandN_i is the corresponding interpolating function associated with node '*i*'.

The total strain energy of the CNTRC plate can be expressed as:

$$U = \frac{1}{2}\iint\left[\int_{-h/2}^{+h/2} \{\varepsilon\}^T [Q]\{\varepsilon\}\, dz\right] dxdy \tag{16}$$

Now, Eq. (16) can be rewritten by substituting the strainfromEqs. (6) and conceded as:

$$U = \frac{1}{2}\iint\left(\{\bar{\varepsilon}\}^T [D]\{\bar{\varepsilon}\}\right) dxdy \tag{17}$$

where, $[D]=\int_{-h/2}^{+h/2}[T]^T\left[Q_{ij}\right][T]dz$.

The total work done by externally applied load (p) and in-plane thermal load is given by

$$W=\iint\{\lambda_0\}^T\{p\}dxdy+\iint\left(\{\varepsilon\}^T[Q]\{\varepsilon_{th}\}\right)dxdy$$

$$W=\{\lambda_0\}^T\{F_m\}+\{\lambda_0\}^T\{F_{th}\} \tag{18}$$

where, $\{F_m\}$ and $\{F_{th}\}$ are the mechanical and thermal load vectors, respectively.

The kinetic energy of the CNTRC plate can be expressed as:

$$T=\frac{1}{2}\int_V\rho\{\dot{\lambda}\}^T\{\dot{\lambda}\}dV \tag{19}$$

where, ρ and $\{\dot{\lambda}\}$ are the mass density and the global velocity vector.

Using, Eqs. (3) and (19), the kinetic energy expression of the CNTRC plate with thickness h can be written as:

$$T=\frac{1}{2}\int_A\left(\int_{-h/2}^{+h/2}\{\dot{\lambda}_0\}^T[f]^T\rho[f]\{\dot{\lambda}_0\}dz\right)dA=\frac{1}{2}\int_A\{\dot{\lambda}_0\}^T[m]\{\dot{\lambda}_0\}dA \tag{20}$$

where, $[m]=\int_{-h/2}^{+h/2}[f]^T\rho[f]dz$ is the inertia matrix.

2.2. ANSYS model and solution steps

As discussed earlier, a simulation model has been developed in ANSYS using APDL code to compute the desired bending and the free vibration responses of the CNTRC plate under thermal environment. The present model is discretized using eight node serendipity element (SHELL281) with six degrees of freedom at each node from the ANSYS element library. The SHELL281 element is capable of solvingthe thick/thin panel under combined thermo-mechanicalload. The solution procedure used in the ANSYS are as follows:

(i) The first step is to create the desired geometry of the plate with sides *a* and*b*.
(ii) Assign the material properties.
(iii) Discretize the plate model using SHELL281 element, from ANSYS element library, to obtain the required mesh.
(iv) Then, apply the boundary condition and the load to get the required responses.
(v) The linear eigenvalue vibration problem is solved using Block Lanczos method.

2.3. Bending analysis

The final form of the governing equation of the CNTRC plate is obtained using variational principle and conceded as:

$$\delta\prod=\delta U-\delta W=0 \tag{21}$$

where, δ is the variational symbol and $\prod$ is the total potential energy.

Now, the desired governing equation for the static analysis of the CNTRC plate is obtained by substituting the values of the strain energy and total work done from the Eqs. (17) and (18) in the Eq. (21) and rewritten as:

$$[K_S]\{\lambda_0\} = \{p\} \tag{22}$$

where, $[K_S]$ is the global stiffness matrix.

2.4. Free vibration analysis

The governing equation of free vibrated CNTRC plate is derived using Hamilton's principle and expressed as:

$$\delta\int_{t_1}^{t_2}(T-U)\,dt = 0 \tag{23}$$

The equilibrium equation for vibrated CNTRC plate can be obtained by substituting the values of the kinetic energy (T) and the strain energy (U) in Eq. (23) and modified as follows:

$$[M]\{\ddot{\lambda}\} + [K]\{\lambda\} = 0 \tag{24}$$

where, $[M] = [N]^T[m][N]$ is the system mass matrix and $[K] = [B]^T[D][B]$ is the system stiffness matrix.

Again, Eq. (24) is rewritten in the eigenvalue equation form and represented as:

$$\left([K] - \omega^2[M]\right)\Delta = 0 \tag{25}$$

where, ω is the natural frequency and Δ is the corresponding eigenvector.

Table 1. Material properties of (10, 10) SWCNT (L= 9.26 nm, R=0.68 nm, h=0.067 nm, v_{12}^{CNT} = 0.175). [28]

Temperature (K)	E_{11}^{CNT} (TPa)	E_{22}^{CNT} (TPa)	G_{12}^{CNT} (TPa)	α_{11}^{CNT} (10^{-6}/K)	α_{22}^{CNT} (10^{-6}/K)
300	5.6466	7.0800	1.9445	3.4584	5.1682
400	5.5679	6.9814	1.9703	4.1496	5.0905
500	5.5308	6.9348	1.9643	4.5361	5.0189
700	5.4744	6.8641	1.9644	4.6677	4.8943

Table 2. Effective parameter of CNT. [28]

V_{CNT}	η_1	η_2	η_3
0.12	0.137	1.022	0.7185
0.17	0.142	1.626	1.138
0.28	0.141	1.585	1.109

3. Results and Discussions

The free vibration and bending behaviour of the CNTRC plate are investigated using suitable finite element model developed in MATLABenvironment. For the present analysis, PMMAis considered as the matrix phase and the SWCNT as the fibre phase.The material properties of both matrix and fibre are assumed to be temperature-dependent. The properties of PMMA are taken same as[28]ρ^m =1150kg/m^3, $v^m = 0.34$,E^m = (3.52-0.0034T) GPa. andα^m = 45(1+0.0005 ΔT) ×10^{-6} in which ΔT= T –

T_0 and T_0= 300K (ambient temperature). Similarly, the properties of the armchair (10, 10) configuration of the SWCNTs is taken same as the reference [28] and presented in Table 1. The effectiveness parameters of CNT isalso provided in Table 2and the effective material properties of the composite plate are obtained using the extended rule of mixture.It is true that the extended rule of mixture is one of the appropriate methodfor the analysis of the short fibre reinforced composite structure. Table 3 shows comparison study of the elastic properties computed using the extended rule of mixture and compared with MD simulation results. It is clear from the table that the present results are showing very good agreement and MD simulation is well accepted in materials related analysis due to its accuracy. In the present analysis,the thickness of the composite plate is taken as 2mm throughout if not stated otherwise.

Table 3. Comparison of effective material properties of the CNT/PMMA composite.

V_{CNT}	MD [2]		Extended rule of mixture	
	E_{11} (GPa)	E_{22} (GPa)	E_{11}(GPa)	E_{22} (GPa)
0.12	94.6	2.9	95.021	2.8917
0.17	138.9	4.9	138.38	4.8776
0.28	224.2	5.5	224.72	5.4807

The following sets of support conditions are employed to compute the desired responses:

(a) All edges simply supported condition (SSSS):

$v = w = \varphi_y = \psi_y = \theta_y = 0$ at $x = 0, a$

$u = w = \varphi_x = \psi_x = \theta_x = 0$ at $y = 0, b$

(b) All edges clamped condition (CCCC):

$u = v = w = \varphi_x = \varphi_y = \psi_x = \psi_y = \theta_x = \theta_y = 0$ for both end i.e., $x = 0, a$ and $y = 0, b$.

(c) Combine simply support and clamped condition (SCSC)

$v = w = \varphi_y = \psi_y = \theta_y = 0$ at $x = 0, a$ and

$u = v = w = \varphi_x = \varphi_y = \psi_x = \psi_y = \theta_x = \theta_y = 0$ at $y = 0, b$.

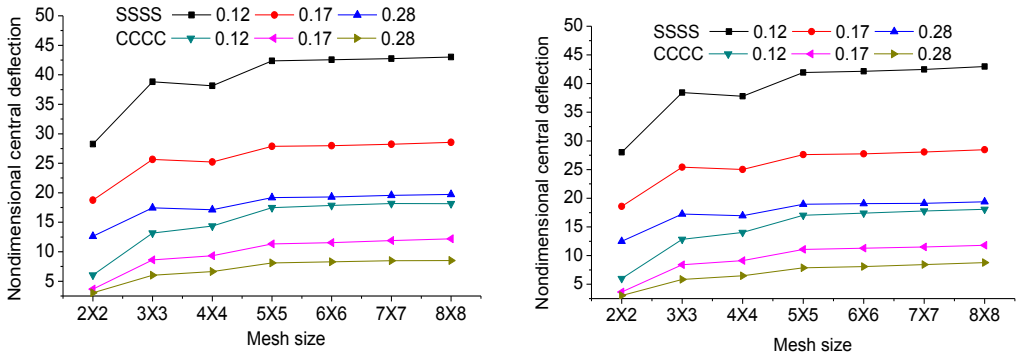

Model 1 Model 2

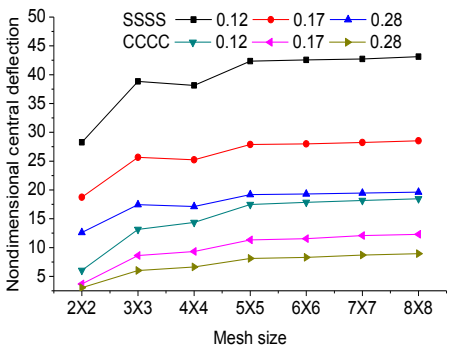

Model 3

Fig. 2:- Convergence behavior of the nondimensional central deflection: (a) Model 1 (b) Model 2 and (c) Model 3.

In this present analysis, the nondimensional form of the central deflection and the frequencies are obtained using the formulae: $\overline{W} = W_{\max} / h$ and $\overline{\omega} = \omega(a^2 / h)\sqrt{\rho_0 / E_0}$ respectively, where E_0, ρ_0 and $W_{max}$are the Young's modulus and the density of the matrix material at ambient temperature (300K) and the maximum central deflection of the plate, respectively.

3.1. Convergence and validation study

In this section, the convergence behaviour of the present numerical models of the CNTRC plate is computed for different support conditions and volume fractions. The convergence behaviour of the nondimensional central deflection parameter and the nondimensional fundamental frequencies of the CNTRC plate is presented in fig. 2(a)-(c) and fig. 3(a)-(c), respectively. In this example, the responses are computed for two support conditions (SSSS and CCCC) and three volume fraction (V_{CNT} = 0.12, 0.17 and 0.28) at room temperature (300K). The nondimensional central deflections are obtained under point load of 10KN at the center of the plate. It is clearly observed from the figures that the present results are converging well with mesh refinement for all the volume fractions and the support conditions. Therefore, a (6×6) mesh is utilized to compute the further analysis.

Now the proposed finite element model is extended to show the validation behaviour by comparing the responses with the available published literature and the simulation model. The nondimensional bending and vibration responses of the clamped CNTRC plate is computed and presented in Table 4 and Table 5, respectively. From results, it is clear that the presently developed models are good agreement with the previously published results. For the comparison purpose all the geometrical and material properties are taken same as to the Zhu *et al.*[18].

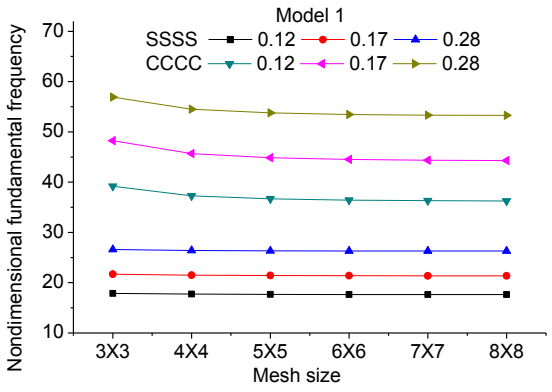

(a) Model 1

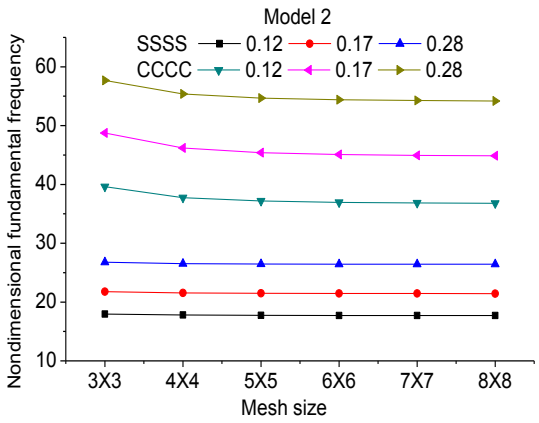

(b) Model 2

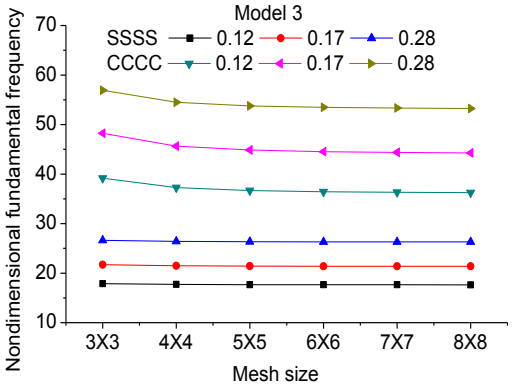

(c) Model 3

Fig. 3:- Convergence behavior of the nondimensional fundamental frequency: (a) Model 1 (b) Model 2 and (c) Model 3.

Table 4.Comparison study of nondimensional central deflection of CNTRC plate (T = 300K and uniformly distributed load = 0.1MPa).

a/h	V_{CNT}	Model 1	Model 2	Model 3	ANSYS	Zhu *et al*. [18]
10	0.11	0.0021	0.0017	0.0021	0.00222	0.0022
	0.14	0.0020	0.0016	0.0020	0.00210	0.0021
	0.17	0.0014	0.0011	0.0013	0.00199	0.0014
20	0.11	0.0134	0.0111	0.0132	0.01335	0.0134
	0.14	0.0118	0.0097	0.0117	0.01190	0.0119
	0.17	0.0085	0.0071	0.0085	0.01090	0.0086

Table 5.Comparison study of nondimensional fundamental frequencies of square CNTRC plate (T =300K)**.**

a/h	V_{CNT}	Model 1	Model 1	Model 2	ANSYS	Zhu *et al*. [18]
10	0.11	18.0904	18.5970	16.5539	17.6385	17.625
	0.14	18.6661	19.2038	17.0819	18.1493	18.127
	0.17	22.5748	23.2008	20.6588	22.0240	22.011
50	0.11	40.0976	37.7016	36.4986	39.6704	39.730
	0.14	43.8828	41.4403	39.9825	43.5893	43.583
	0.17	49.5328	46.5099	45.0802	48.9897	49.074

Table 6. Effect of volume fraction on the nondimensional central deflection.

Support conditions	Load (KN)	V_{CNT}= 0.12			V_{CNT}= 0.17			V_{CNT}= 0.28		
		Model 1	Model 2	Model 3	Model 1	Model 2	Model 3	Model 1	Model 2	Model 3
SSSS	2	8.511	8.430	8.511	5.598	5.550	5.598	3.859	3.482	3.859
	4	17.021	16.859	17.021	11.195	11.101	11.195	7.717	6.963	7.717
	6	25.532	25.289	25.532	16.793	16.651	16.793	11.576	10.445	11.576
	8	34.042	33.719	34.042	22.391	22.202	22.391	15.435	13.927	15.435
	10	42.553	42.148	42.553	27.989	27.752	27.989	19.293	17.409	19.293
CCCC	2	3.568	3.482	3.568	2.308	2.258	2.308	1.661	1.614	1.662
	4	7.137	6.963	7.137	4.616	4.515	4.616	3.323	3.229	3.323
	6	10.705	10.445	10.705	6.924	6.773	6.924	4.984	4.843	4.985
	8	14.274	13.927	14.274	9.232	9.031	9.232	6.646	6.457	6.646
	10	17.842	17.409	17.842	11.540	11.289	11.540	8.307	8.072	8.308
SCSC	2	8.394	8.317	8.394	5.481	5.436	5.481	3.835	3.793	3.835
	4	16.789	16.633	16.789	10.963	10.873	10.963	7.670	7.585	7.670
	6	25.183	24.950	25.183	16.444	16.309	16.444	11.505	11.378	11.505
	8	33.578	33.266	33.578	21.926	21.745	21.926	15.341	15.170	15.341
	10	41.972	41.583	41.972	27.407	27.182	27.407	19.176	18.963	19.176

3.2. Parametric Study

Based on the convergence and comparison study, the developed higher-order CNTRC plate model is extended to compute the responses for the different geometrical and material parameters. The effect of various parameters on the flexural and free vibration behaviouris discussed in detailed. In general the responses are computed for a/h = 50, V_{CNT} =0.12 anda/b = 1 at 300K throughout the analysis if not

stated otherwise. For the computational purpose, the thickness of the composite panel is taken as h = 0.002 m and discussed in detailed.

3.2.1. Flexural behaviour

In this section, flexural behaviour of CNTRC panel is investigated for different geometrical and material parameters. The effect of the CNT volume fractions on the bending responses of the square CNTRC plate is examined for three volume fractions (V_{CNT} = 0.12, 0.17 and 0.28), five point loads (p = 2, 4, 6, 8, and 10KN) at the center with three support conditions (SSSS, CCCC and SCSC) and presented in Table6. It is clearly observed from the figures that the nondimensional central deflections are increasing with externally applied load and decreasing with the volume fractions of the CNT.

The thickness ratio of any structural component playsan important role on the stiffness behavior of the structure. The effect of five thickness ratios (a/h = 10, 20, 30, 40 and 50) on the nondimensional central deflections of the square CNTRC plate are examinedfor two volume fraction (V_{CNT} = 0.12 and 0.17) and three support conditions (SSSS, CCCC and SCSC) with point load (p=10KN) at the center point of the composite plateand presented in Table 7. It can be seen that the nondimensional central deflections are increasing with thickness ratios of CNTRC plate.

Table 7. Effect of thickness ratio on the nondimensional central deflection.

		V_{CNT} = 0.12			V_{CNT} = 0.17		
	a/h	Model 1	Model 2	Model 3	Model 1	Model 2	Model 3
SSSS	10	4.9587	4.6417	4.9587	3.0398	2.8504	3.0398
	20	10.0051	9.6305	10.0051	6.3644	6.1432	6.3644
	30	17.9343	17.5405	17.9344	11.6228	11.3918	11.6229
	40	28.7761	28.3745	28.7761	18.8273	18.5925	18.8273
	50	42.5531	42.1482	42.5531	27.9887	27.7522	27.9887
CCCC	10	4.0394	3.7729	4.0394	2.4268	2.2644	2.4269
	20	6.2431	5.8627	6.2431	3.8452	3.6192	3.8453
	30	9.2030	8.7840	9.2030	5.7963	5.5505	5.7963
	40	13.0553	12.6239	13.0553	8.3543	8.1031	8.3543
	50	17.8422	17.4087	17.8423	11.5402	11.2887	11.5403
SCSC	10	4.7813	4.4959	4.7814	2.9159	2.7464	2.9160
	20	9.8152	9.4615	9.8152	6.2033	5.9967	6.2033
	30	17.6576	17.2812	17.6577	11.3652	11.1467	11.3652
	40	28.3673	27.9817	28.3674	18.4284	18.2053	18.4284
	50	41.9723	41.5829	41.9724	27.4070	27.1818	27.4071

The CNT is well known for its good thermal property, and it becomes more significant when the structure is exposed to the elevated temperature field. In this present example, the CNT properties are assumed to be temperature-dependent, and, therefore, environmental temperature plays a significant role on the flexural strength of the CNTRC plate. The nondimensional central deflections of the square CNTRC plate are analyzed for three different temperature loading (T = 300K, 500K and 700K), three support conditions (SSSS, CCCC and SCSC) by varying the value of point load andpresented in Table 7. It is observed that the nondimensional central deflections of the CNTRC plate are increasing as the temperature load increase.

The deformation behaviour of the CNTRC plate is computed for model 1 and model 2 with three support condition (SSSS, CCCC and SCSC) and presented in fig. 4 (a)-(f). The responses are computed by setting a/h = 50, V_{CNT} = 0.12 and p= 10KN at room temperature (T = 300K). It is clearly observed that the deformation of the plate is maximum and minimum for the SSSS and the CCCC support conditions, respectively and the responses are within the expected line.

Table8. Effect of temperature on the nondimensional central deflection.

Support Conditions	Load (KN)	Temperature (K)								
		300			500			700		
		Model 1	Model 2	Model 3	Model 1	Model 2	Model 3	Model 1	Model 2	Model 3
SSSS	2	8.5106	8.4296	8.5106	9.0049	8.9099	9.0049	9.5673	9.4526	9.5673
	4	17.0212	16.8593	17.0212	18.0097	17.8197	18.0097	19.1346	18.9053	19.1346
	6	25.5318	25.2889	25.5319	27.0146	26.7296	27.0146	28.7018	28.3579	28.7019
	8	34.0425	33.7185	34.0425	36.0194	35.6395	36.0195	38.2691	37.8106	38.2691
	10	42.5531	42.1482	42.5531	45.0243	44.5493	45.0243	47.8364	47.2632	47.8364
CCCC	2	3.5685	3.4817	3.5685	3.8354	3.7331	3.8354	4.1621	4.0381	4.1621
	4	7.1369	6.9635	7.1369	7.6708	7.4663	7.6708	8.3243	8.0761	8.3243
	6	10.7054	10.4452	10.7054	11.5062	11.1994	11.5062	12.4864	12.1142	12.4864
	8	14.2738	13.9270	14.2738	15.3416	14.9326	15.3416	16.6486	16.1522	16.6486
	10	17.8423	17.4087	17.8423	19.1770	18.6657	19.1770	20.8107	20.1903	20.8107
SCSC	2	8.3945	8.3166	8.3945	8.9255	8.8334	8.9255	9.5240	9.4118	9.5240
	4	16.7889	16.6332	16.7889	17.8510	17.6668	17.8510	19.0480	18.8236	19.0480
	6	25.1834	24.9497	25.1834	26.7765	26.5001	26.7765	28.5720	28.2354	28.5720
	8	33.5779	33.2663	33.5779	35.7020	35.3335	35.7020	38.0960	37.6472	38.0960
	10	41.9723	41.5829	41.9724	44.6275	44.1669	44.6275	47.6200	47.0590	47.6200

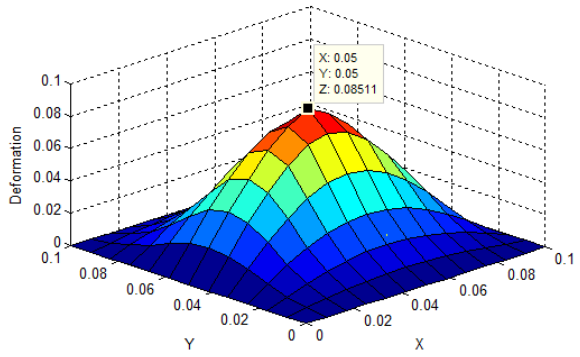

(a) Model 1, SSSS

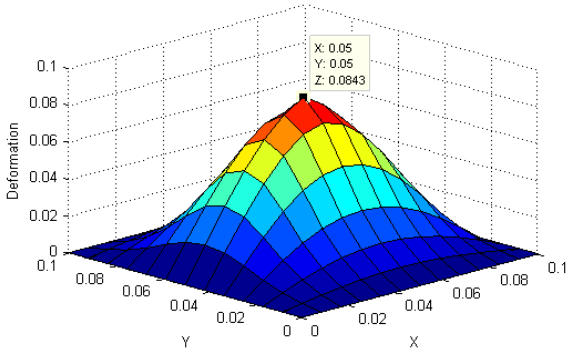

(b) Model 2, SSSS

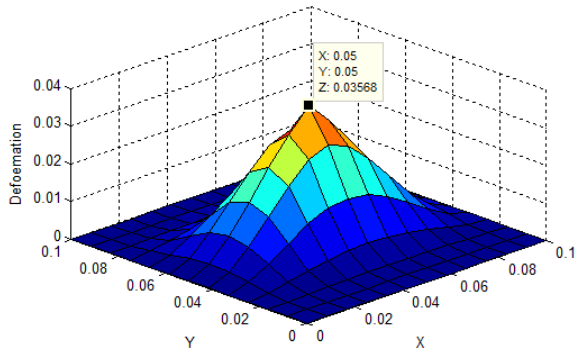

(c) Model 1, CCCC

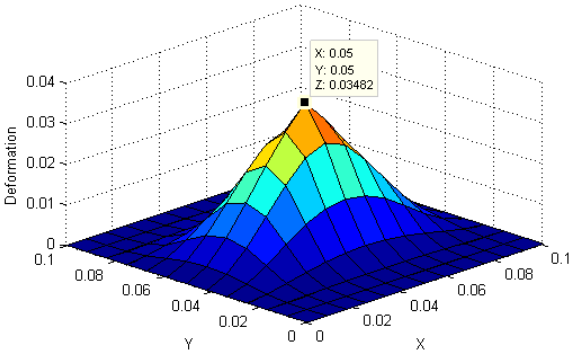

(d) Model 2, CCCC

Fig. 4:- Deformed configuration of CNTRC panel: (a) Model 1, SSSS, (b) Model 2, SSSS, (c) Model 1, CCCC and (d) Model 2, CCCC.

3.2.2. Vibration and modal analysis

In this section, the effect of different geometrical and material parameters on the free vibration responses are examined using the developed three micromechanical finite element model of the CNTRC plate. In general, the responses are examined for T = 300K V_{CNT} = 0.12 and a/h = 50 throughout the analysis if not stated otherwise.

It is well known that the volume fraction of the CNT plays a significant role in stiffness response of the CNTRC plate. The effect of volume fractions (V_{CNT} = 0.12, 0.17 and 0.28) of the CNT on the nondimensional fundamental frequencies of the square CNTRC plate is analyzed usinga/h =50 under two temperature (T = 300K and 400K) load. The nondimensional fundamental frequency of the CNTRC plate is computed and presented in Table9 for three support conditions (SSSS, CCCC and SCSC). It is clearly observed that the nondimensional fundamental frequencies are increasing with the volume fractions of the CNT and decreasing with the temperature.

Table 9. Effect of volume fraction on the nondimensional fundamental frequency.

	V_{CNT}	T=300K			T=400K		
		Model 1	Model 2	Model 3	Model 1	Model 2	Model 3
SSSS	0.12	17.6564	17.7262	17.6563	17.3654	17.4427	17.3651
	0.17	21.3910	21.4649	21.3910	21.0425	21.1245	21.0425
	0.28	26.3164	26.4439	26.3163	25.9105	26.0522	25.9104
CCCC	0.12	36.4265	36.9554	36.4264	35.51	36.0831	35.5101
	0.17	44.5219	45.0966	44.5245	43.4643	44.0877	43.4651
	0.28	53.4669	54.3944	53.4666	52.0619	53.062	52.0617
SCSC	0.12	18.9113	18.9813	18.9125	18.4697	18.5471	18.4698
	0.17	23.1087	23.1871	23.1118	22.5583	22.6404	22.5601
	0.28	27.8613	27.9886	27.8616	27.2702	27.4090	27.2683

In this present analysis, the material properties of the CNTand the matrix are assumed to be temperature-dependent,therefore,the temperature field effect on the vibration behaviour of the CNTRC plate is investigated. Fig.5(a) and (b) shows the nondimensional fundamental frequency of the square CNTRC plate under fourdifferent temperature loads (T=300K, 400K, 500K and 700K), two support conditions (SSSS and CCCC), and three volume fractions of CNT (V_{CNT}). It is observed that the nondimensional fundamental frequency responses of the CNTRC plate decrease as the temperature load increases for all type support conditions.

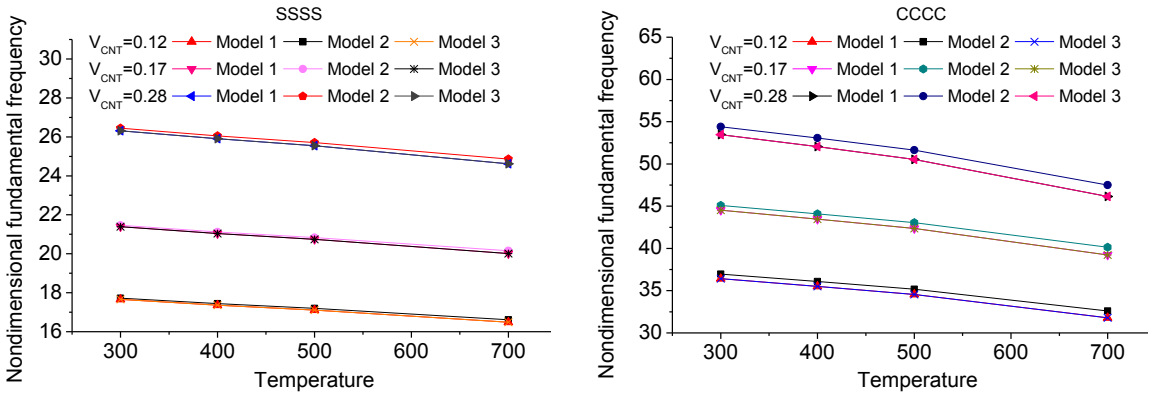

(a) SSSS (b) CCCC

Fig. 5:- Effect of temperature on the nondimensional fundamental frequency: (a) SSSS and (b) CCCC.

In this example, the effect of thickness ratios on the nondimensional fundamental frequency of CNTRC square plate is examined. The responses are computed for five thickness ratios (a/h = 10, 20, 30, 40 and 50) and two support conditions (SSSS and CCCC) under two uniform thermal loads (T = 300K and 700K) with V_{CNT} =0.12 and plotted in fig.6 (a) and (b).It is observed that the nondimensional fundamental frequencyis increasedwith the volume fractions of the CNT. Moreover, the nondimensional fundamental frequency increase sharply with increase the thickness ratio but the rate of increase reduces for thehigher value of thickness ratio.

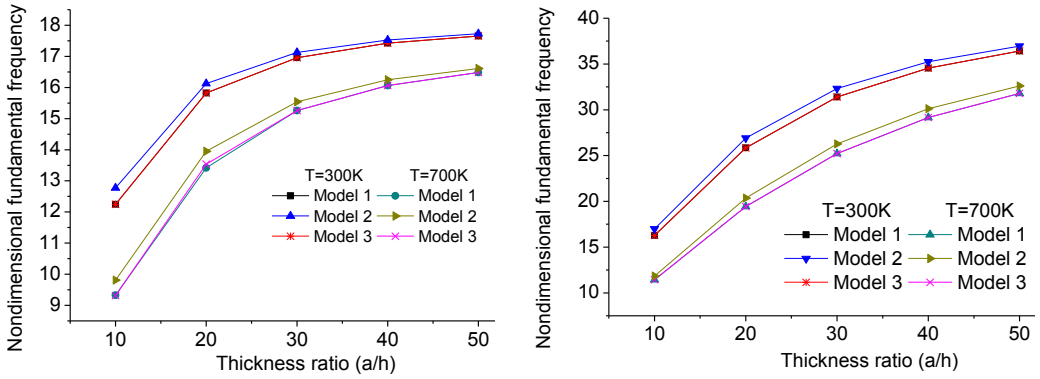

(a) SSSS (b) CCCC

Fig. 6:- Effect of thickness ratio (a/h) on the nondimensional fundamental frequency: (a) SSSS and (b) CCCC.

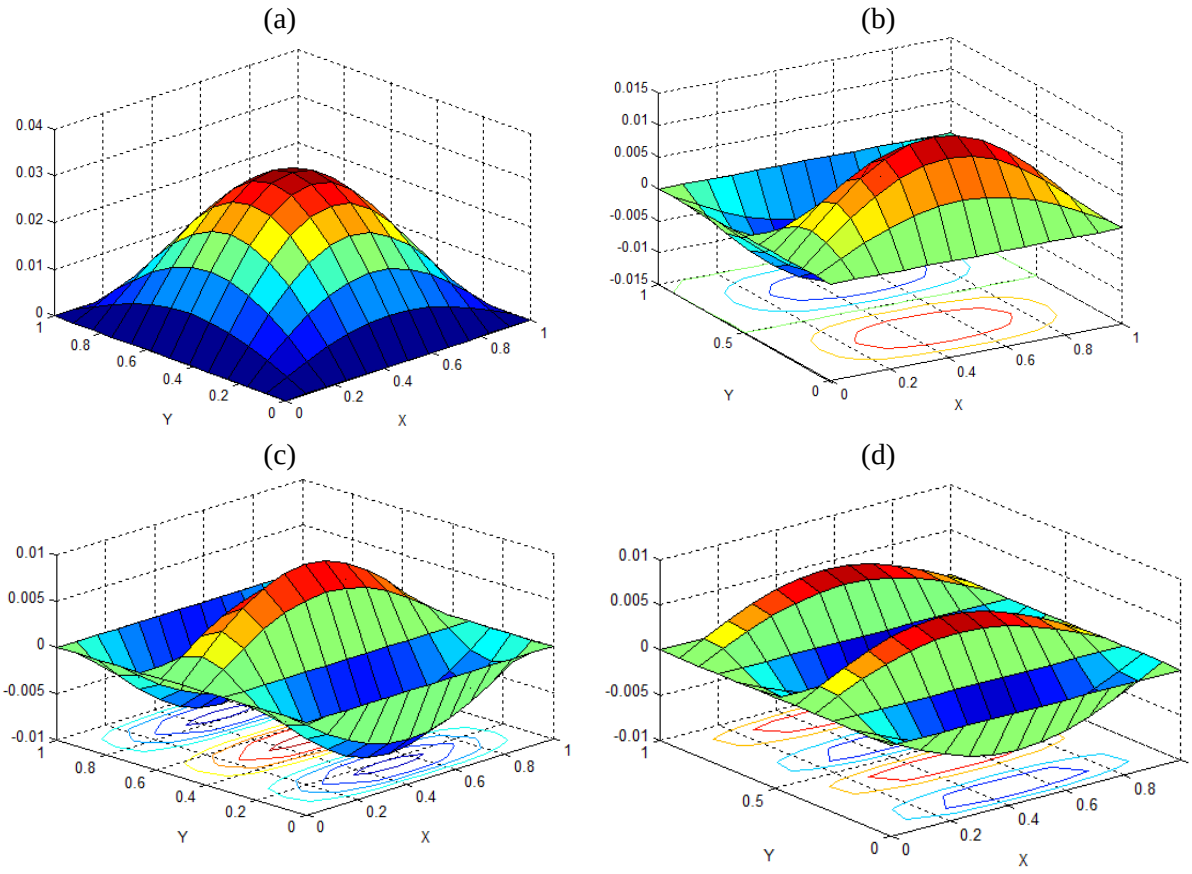

Fig.7:- Free vibration mode shapes of a simply supported uniformly distributed CNTRC square plate (Model-1): (a) 1st Mode (b) 2nd Mode (c) 3rd Mode (d) 4th Mode.

Fig. 7(a)-(d) represent the four mode shapes of the square clamped CNTRC plate (Model 1) at ambient temperature (T = 300K) by setting the geometrical parameters as a/h = 50 and V_{CNT} = 0.12. It is well known that the mode shapes are not giving any numerical value rather it provides the direction of vibration and the present responses are following the expected line.

4. Conclusions

In the present article, the free vibration and bending responses of the SWCNT reinforced composite plate are computed using the FSDT and HSDT mid-plane kinematics in conjunction with the FEM under uniform thermal environment. To achieve the realistic behaviour, the material properties of both (CNT and matrix) are assumedto be temperature dependent.The CNTs are uniformly distributed with respect to the dimension of the plate, and the effective material properties of the composite are computed using the extended rule of mixture. The desired governing equation of bending and free vibration are obtained using the suitable FEM steps. The responses are computed numerically using the suitableFEM steps with the help of ninenodedisoparametricelements with nine (model 1), six (model 2)and ten (model 3) DOFseachnode. The present models are showing good convergence rate with mesh refinement. The comparison study also indicates the validity of the present first and higher order models. The models arealso validated by comparing the responses of the simulation model developed in ANSYS using APDL code. The effect of the different geometrical and material parameters on the free vibration and bending under thermal environment are computed.The following conclusions are drawn from the detailed parametric study.

(i) The convergence and comparison study shows the accuracy of the present FSDT and HSDT models with and without temperature load.

(ii) The nondimensional central deflections are increasing with the rise of the mechanical load, temperature load and the thickness ratio. However, the deflections are showing a reverse trend for the volume fraction.

(iii) The nondimensional fundamental frequency is increasing with the increasein the volume fractionand the thickness ratios. However, the nondimensional frequency is showing a reverse trend for the temperature load.

(iv) The results indicated that the FSDT model (Model 2) is the stiffest configuration as compared to the HSDT models (Model 1 and Model 3).

Appendix

$$\{\lambda\}=\{u\ v\ w\}^T,\{\lambda_{01}\}=\left[u_0\ \ v_0\ \ w_0\ \ \varphi_x\ \ \varphi_y\ \ \psi_x\ \ \psi_y\ \ \theta_x\ \ \theta_y\right]^T,\{\lambda_{02}\}=\left[u_0\ \ v_0\ \ w_0\ \ \varphi_x\ \ \varphi_y\ \ \varphi_z\right]^T$$

$$\{\lambda_{03}\}=\left[u_0\ \ v_0\ \ w_0\ \ \varphi_x\ \ \varphi_y\ \ \varphi_z\ \ \psi_x\ \ \psi_y\ \ \theta_x\ \ \theta_y\right]^T$$

$$[f_1]=\begin{bmatrix}1&0&0&z&0&z^2&0&z^3&0\\0&1&0&0&z&0&z^2&0&z^3\\0&0&1&0&0&0&0&0&0\end{bmatrix},\ [f_2]=\begin{bmatrix}1&0&0&z&0&0\\0&1&0&0&z&0\\0&0&1&0&0&z\end{bmatrix},$$

$$[f_3]=\begin{bmatrix}1&0&0&z&0&0&z^2&0&z^3&0\\0&1&0&0&z&0&0&z^2&0&z^3\\0&0&1&0&0&z&0&0&0&0\end{bmatrix}$$

References

[1] Moradi-Dastjerdi R, Pourasghar A, ForoutanM and Bidram M 2014*J Compos Mater***48**1901-1913.
[2] Han Y, Elliott J 2007*Comput Mater Sci***39**315–23.
[3] Shen H S and Zhu Z H 2012*Eur J Mech A-Solid***35**10-21.
[4] Liu Y J and Chen X L 2003 *Mech Mater***35**69-81.
[5] Chen X L and Liu Y J 2004*Compos Mater Sci***29**1-11.
[6] Alibeigloo A 2013*Comp Struct***95**612-22.
[7] Lin Fand Xiang Y 2014*Appl Math Model***38**3741–3754.
[8] LiewK M, LeiZ X,Yu J LandZhangL W2014 *Comput Methods ApplMechEngrg***268**1-17.
[9] AyatollahiaM R, ShadlouS and ShokriehM M 2011*Compos Struct***93**2250-2259.
[10] Aragh B S, FarahaniE B and Barati A H N 2012*Math Mech Solids***18** 264-284.
[11] Lin F and Xiang Y 2014*International Journal of Structural Stability and Dynamics* DOI:10.1142/S0219455413500569
[12] Shen Z B, Sheng L P and Li X F 2012*Physica E***44** 1169-1175.
[13] Ke L L, Yang J and Kitipornchai S 2013*Mechanics of Advanced Materials and Structures***22**28-37.
[14] AlvaA and Raja S 2014*Mechanics of Advanced Materials and Structures***21**197-206
[15] Jarali S, PatilS F and Pilli S C 2015*Mechanics of Advanced Materials and Structure***22** 428-439.
[16] VodenitcharovaT and Zhang L C 2006*Int J Solids Struct***43**3006-3024.
[17] Formica G, LacarbonaraWand Alessi R 2010 *J Sound Vib***329**1875-1889.
[18] Zhu Z H, Lei Z X and Liew K M 2012 *Compos Struct***94**1450-1460.
[19] YasM H and Heshmati M 2012*Appl Math Model***36**1371-1394.
[20] Lei Z X, Yu J L and Liew K M 2013 *International Journal of Materials Science and Engineering***1**36-40.
[21] Lei Z X, LiewK M and Yu J L 2013*Compos Struct***106**128-138.
[22] Lei Z X, LiewK M and Yu J L 2013*Compos Struct***98**160-168.
[23] AlibeiglooAand Liew K M 2013 *ComposStruct***106** 873-881.
[24] Lei Z X, Zhang L W, LiewK M and Yu J L 2014*Compos Struct***113**328-338.
[25] MehrabadiS J and Aragh B S 2014*Thin WallStruct***80**130-41.
[26] Kishore M D V H, Singh B N and Pandit M K 2011*AerospSciTechnol***15** 224-235.
[27] Szekrenyes A 2014 *J Compos Mater***48** 1441-1457.
[28] Shen H S and Xiang Y 2013*EngStruct***56** 698-708.